Desalination and Water Treatment
www.deswater.com

doi: 10.5004/dwt.2020.25380

185 (2020) 175–184
May

The adsorption kinetic parameters of Cu^{2+} and Cr^{3+} ions by α-C_2SH

Domante Niuniavaite*, Kestutis Baltakys, Tadas Dambrauskas

Department of Silicate Technology, Kaunas University of Technology, Radvilenu Road 19, LT-50270 Kaunas, Lithuania, Tel. +370-73-300163; emails: domante.niuniavaite@ktu.edu (D. Niuniavaite), kestutis.baltakys@ktu.lt (K. Baltakys), tadas.dambrauskas@ktu.lt (T. Dambrauskas)

Received 5 February 2019; Accepted 22 December 2019

ABSTRACT

Due to high toxicity, heavy metal ions may cause serious ecological and environmental problems. Thus, in this study, the adsorption capacity and selectivity of synthetic α-C_2SH for Cu^{2+} and Cr^{3+} ions were examined. The adsorbent was synthesized under hydrothermal conditions at 175°C, when the molar ratio of the primary mixture was $CaO/SiO_2 = 1.5$ and the duration of isothermal curing was 24 h. To determine the adsorption capacity of α-C_2SH for Cu^{2+} and Cr^{3+}ions, the batch method was employed: initial metal ions concentration varied from 0.25 to 10 g/L, while the reaction temperature and duration were equal to 25°C and 30 min. The adsorption experiments showed that α-C_2SH adsorption capacity for Cu^{2+} and Cr^{3+} ions were equal to 615.54 and 241.42 mg/g, respectively. The obtained results were confirmed by X-ray diffraction, simultaneous thermal analysis, AAS analysis and kinetic calculations.

Keywords: Calcium silicate hydrate; α-C_2SH; Adsorption; Heavy metals; Kinetics

1. Introduction

Heavy metals are significant environmental pollutants and their toxicity is a reason for increasing ecological, evolutionary, nutritional, and environmental problems [1–5]. These metals are mainly discharged in industrial wastewater due to mining operations, battery manufacturing processes, the production of paints and pigments [6–8]. It is worth indicating that the aforementioned pollutants are highly soluble in aquatic environments and, as a consequence, they can be absorbed by living organisms and may accumulate in the human body [1,9–13]. For this reason, heavy metals should be prevented from reaching the natural environment. To remove pollutants from water systems, the conventional technologies such as chemical precipitation, ion exchange, electrochemical treatment, coagulation, foam flotation, filtration, aerobic and anaerobic treatment, solvent extraction, activated sludge, adsorption, and others are used [6,7,14,15]. Among these techniques, adsorption offers flexibility in design and operation. In many cases, it generates high-quality treated effluents. In addition, mineral, organic or biological origin zeolites and other materials with the high surface area can be used as adsorbents [16–21]. However, these materials often have a low adsorption capacity (Table 1), poor regeneration (metal ion removal) and short lifetime. Due to poor adsorbent properties, this process becomes expensive and economically useless. Therefore, researchers are investigating and searching for new, promising materials [22–24].

Nowadays, the interest in calcium silicate hydrates is increasing [29,30] because these compounds can resolve various environmental problems such as energy consumption and CO_2 emissions (if they are used as alternative cementitious materials [31,32]) and water pollution by toxic heavy metal ions (if they are used as adsorbents [33,34]). Calcium silicate hydrates can be either found in nature or cement stone or synthesized by a hydrothermal method in CaO and SiO_2 mixtures [35,36]. The properties and alkalinity of the

---

* Corresponding author.

Table 1
Different adsorbents capacity to heavy metals adsorption [25–28]

	Heavy metal		Adsorption		
Adsorbent	Ion	Initial concentration, g/L	Time, min	Adsorbed concentration, mg/g	k_2 (g/(mg min))
Gyrolite	Cu^{2+}	1.00	30	39.24	–
	Co^{2+}	0.25	15	14.66	0.45
	Fe^{3+}	0.25	60	25	1.68
	Ni^{2+}	0.25	60	18.96	1.37
	Zn^{2+}	0.25	60	21.75	1.26
Hydrotalcite	Co^{2+}	0.25	60	20.09	1.10
	Mn^{2+}	0.25	60	16.63	1.35
	Cu^{2+}	1.00	60	31.4	–
	Ni^{2+}	0.25	60	24.39	0.24
	Fe^{3+}	0.25	60	25	3.20
Zeolites	Pb^{2+}	0.10	60	186	–
	Cu^{2+}	0.10	60	10.3	–
	Co^{2+}	0.05	60	34.5	–
	Co^{2+}	0.40	60	140	–
	Zn^{2+}	0.10	30	9	–
	Cd^{2+}	0.25	60	52.82	–
Fly ash zeolite	Zn^{2+}	0.05	240	26.58	0.001
	Co^{2+}	0.05	240	9.34	0.006
	Cu^{2+}	0.10	240	72.04	0.005
	Cr^{3+}	0.10	240	56.41	0.001

mentioned compound depend on the molar ratio and nature of raw materials, hydrothermal synthesis conditions, and other parameters. Mostly, pH values of the mentioned compounds vary from 10 to 13 [37,38].

The ion exchange properties of calcium silicates hydrates depend on their chemical composition and the structure of crystalline lattice [39,40]. Many authors [41,42] have been reported that lower basicity calcium silicate hydrates (gyrolite and tobermorite) act as chemosorbents for Cu, Fe, Zn, Cd, Mn, Cr, and other ions. Gyrolite with incorporated metal ions can be used and utilized as an alternative cementitious material in ordinary Portland cement [43]. It is known that calcium silicate hydrates are stable in the liquid medium which pH values are equal to 4–12. Unlike calcium silicate hydrates, metal ions (Cu^{2+}, Cr^{3+}, Co^{2+}) exist only in acid media because the formation of complex compounds or metal hydroxides proceed in the alkaline solutions. Several studies suggest that it is not expedient to alkaline the nitrate solutions for the following reasons:

- Practical aspects: the wastewater having acidic properties cannot exist in alkaline media because it forms complex compounds [44–46]. For example, when ammonia water is added to the solution (in order to increase pH value), metal ions form complex compounds such as $(Cu(NH_3)_4)(OH)_2$, and the adsorption process is following a much more complicated mechanism [47,48];
- Due to different properties (valence, atom charge) of cations and anions (ammonium, nitrate, etc.);
- Alkaline ions (sodium, ions, etc.) usually block the adsorbent active centers which have a negative impact on the adsorption process [49].

However, there is little data about the adsorption capacity of the dibasic calcium silicate hydrate – α-C_2SH ($Ca_2(SiO_3OH)(OH)$) which is one of the most important compounds in the manufacturing of alternative cementitious materials. In the previous work [50], it was determined that α-C_2SH showed very good adsorption properties for Co^{2+} ions (~99% removal efficiency) and this process depended on the initial concentration of cobalt ions in the liquid medium. As far as it is known, there has been no data on the adsorption properties of α-C_2SH for other metal ions and the influence of their concentration on the stability of α-C_2SH. Thus, this study focuses on the determination of ion exchange capacity and selectivity of synthetic α-C_2SH for Cu^{2+} and Cr^{3+} metal ions in acidic solutions.

2. Materials and methods

Following reagents for the synthesis of α-C_2SH were used: fine-grained $SiO_2{\cdot}nH_2O$, which was grounded for 2.5 min in a vibrating cup ''Pulverisette 9'' mill at 900 rpm speed, (loss on ignition–16.9%) and calcium oxide produced from $Ca(OH)_2$, which was burned at 450°C for 1 h (free CaO–96.42%). The synthesis of the adsorbent was based on the hydrothermal method. The molar ratio of the primary mixture was equal to 1.5, while the temperature and duration of synthesis to 175°C and 24 h, respectively. It was determined that the pH value of the liquid medium was 12.4. The obtained adsorbent consisted of the dibasic calcium silicate–α-C_2SH (PDF04-009-6343) and semicrystalline C–S–H type compounds (PDF00-033-0306 and PDF00-034-0002) (Fig. 1). The detailed descriptions of adsorbent synthesis are available in [18,19,50].

Adsorption experiments were carried out at 25°C temperature in a thermostatic absorber Grant SUB14 by stirring 5 g of synthetic α-C_2SH in 500 mL of $Cu(NO_3)_2\cdot 3H_2O$ or $Cr(NO_3)_3\cdot 9H_2O$ solutions containing 0.25, 1, or 10 g Me^{x+}/dm^3 (where Me is Cu^{2+} and Cr^{3+} ions respectively), when the duration of adsorption varied in a 0.5–30 min range. The experimental conditions were chosen according to the literature [51] which shows that the adsorption temperature does not have any significant influence on the adsorption capacity and process rate because almost all heavy metal ions (up to 90% all metal ions concentration) are adsorbed by synthetic calcium silicates hydrates within 30 s. The concentrations of heavy metal ions were determined using a Perkin-Elmer Analyst 4000 spectrometer (Perkin Elmer, Waltham, MA, USA). The value of pH was measured with a Hanna instrument (Hi 9321, microprocessor pH meter, Hanna Instruments, Woonsocket, RI, USA) (Table 2). The concentration of nitrate anions was determined using a Flow Injection Analyst FIAlyzer-100 (FIAlab Instruments, USA). FIAlyzer-100 system: FIAlyzer-100, integrated FIA LOV manifold, USB4000 UV/VIS spectrometer, HL2000-LL visible tungsten lamp. The obtained samples were characterized by powder X-ray diffraction (XRD; with a D8 Advance X-ray diffractometer), and simultaneous thermal analysis (STA; with a Linseis PT1000 instrument) [18,19,50].

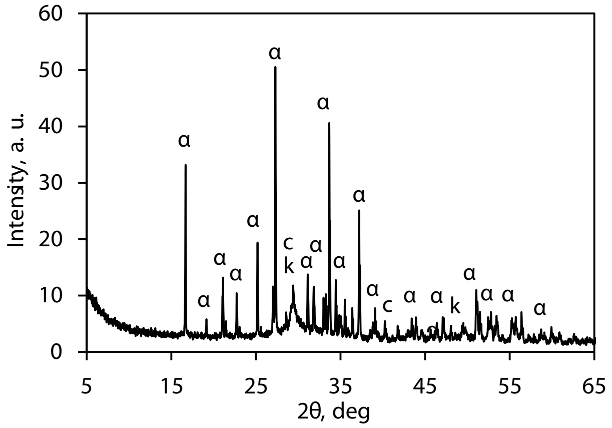

Fig. 1. XRD pattern of synthetic adsorbent. Indexes: α – α-C_2SH; c – $CaCO_3$; k – C-S-H(I)/C-S-H(II).

Table 2
pH values of initial solutions

Initial concentration / Solution	0.25, g Me^{x+}/dm^3	1, g Me^{x+}/dm^3	10, g Me^{x+}/dm^3
		pH value	
$Cu(NO_3)_2\cdot 3H_2O$	6.07	4.72	4.08
$Cr(NO)_3\cdot 9H_2O$	3.57	2.99	2.25

According to the literature, two types of equations, namely the pseudo-first-order (PFO) and the pseudo-second-order (PSO), were commonly used to describe the kinetic models and to study the adsorption systems [16,26,50,52–54]. The PFO kinetic equation proposed by Lagergren for adsorption analysis can be expressed as follows [55]:

$$\frac{dq_t}{dt} = k_1\left(q_e - q_t\right) \tag{1}$$

where q_e and q_t are adsorption capacity at equilibrium and at time t_e, respectively (mg/g), k_1 is the rate constant of PFO adsorption (min^{-1}). After integration and applying boundary conditions $0 \le t \le t_e$ and $0 \le q_t \le q_e$ the integrated form becomes:

$$\log\left(q_e - q_t\right) = \log q_e - \frac{k_1}{2.303}t \tag{2}$$

The PSO adsorption kinetic rate equation is expressed as [56]:

$$\frac{dq_t}{dt} = k_2(q_e - q_t)^2 \tag{3}$$

where k_2 is the rate constant of the PSO adsorption (g/(mg min)). For the boundary conditions $0 \le t \le t_e$ and $0 \le q_t \le q_e$, the integrated form of the equation (the integrated rate law for the PSO reaction) becomes:

$$\frac{t}{q_t} = \frac{1}{kq_e^2} + \frac{1}{q_e}t \tag{4}$$

3. Results and discussion

3.1. Adsorption experiments in 0.25 g Me^{x+}/dm^3 solution

It was observed that the adsorption capacity of α-C_2SH, as well as the intercalation of heavy metals ions in its structure, depends on the chemical nature of adsorbate. As expected, in the lower concentration metal ions solutions (0.25 g/L), the adsorption process proceeded intensively at the beginning, because, after 30 s, all Cu^{2+} (Fig. 2a) and Cr^{3+} (Fig. 2b) ions (25 mg Cu^{2+}/g; 25 mg Cr^{3+}/g) from the primary solution were incorporated into the structure of α-C_2SH. Due to the fast adsorption of the aforementioned ions by the adsorbent, the PFO and PSO equation cannot be used for the description of the process.

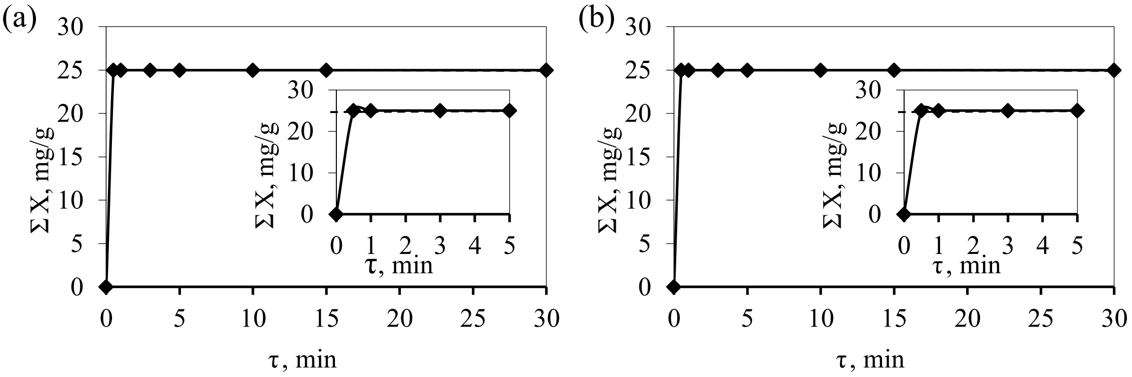

Fig. 2. Integral kinetic curves of Cu^{2+} (a) and Cr^{3+} (b) ions adsorption by α-C_2SH, when the initial concentration of ions was equal to 0.25 g/dm^3.

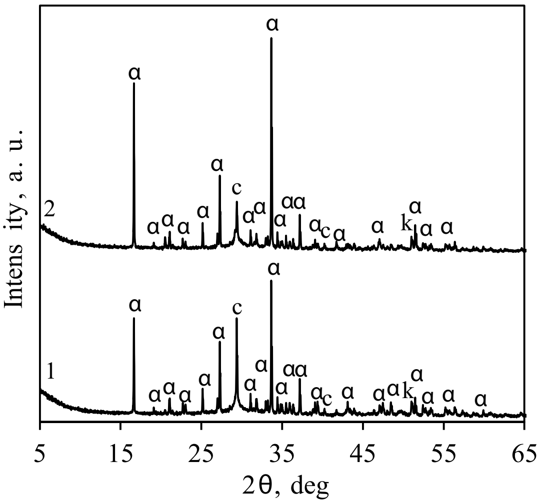

Fig. 3. XRD patterns of α-C_2SH after the adsorption in Cu^{2+} (Curve 1) and Cr^{3+} (Curve 2) solutions, when the initial concentration was equal to 0.25 g/cm^3. Indices: *α* – α-C_2SH; *c* – $CaCO_3$; *k* – C-S-H(I)/C-S-H(II).

To determine whether the adsorption reactions are reversible or irreversible, the saturated adsorbent was dried up and immersed in the distilled water (water to solid ratio–10). The results revealed that, after 30 min, the concentration of metal ions in the liquid medium does not exceed the detection limit. Moreover, during the adsorption, the structure of α-C_2SH remained stable as the intensity of the main diffraction peak (*d*-spacing–0,327 nm) of this compound slightly decreased (Fig. 3).

In brief, α-C_2SH showed good adsorption properties in 0.25 g Cu^{2+} or Cr^{3+}/dm^3 solutions in comparison with other adsorbents [26]. Thus, in the next stage of this work, the adsorption experiment was performed in higher concentration solutions (1 g/cm^3).

3.2. Adsorption experiments in 1.00 g Me^{x+}/dm^3 solution

When the concentration of heavy metal ions in the solution was equal to 1.00 g Me^{x+}/dm^3, the uptake of these ions by the adsorbent proceeded slower (Figs. 2 and 4). Within 30 s of Cu^{2+} ions adsorption, the removal efficiency of α-C_2SH reaches ~73 % (72.91 mg/g) (Fig. 4a). Meanwhile, the quantity of adsorbed Cr^{3+} ions (Fig. 4b) by the latter compound was higher and equal to 86 % (86.14 mg/g). By prolonging the duration of the experiment to 3 min, the adsorbed amount of Cu^{2+} ions slightly increased, however, the removal of these ions was completed only after 30 min (Fig. 4a). In the meantime, the uptake of Cr^{3+} ions reached 100% already after 3 min (Fig. 4b). As in the previous case (0.25 g Me^{x+}/dm^3), it was found that the adsorption process is irreversible because the concentration of heavy metal ions in the liquid medium did not exceed ~0.01%. The obtained results were also confirmed by XRF analysis: 16.1% of Cu^{2+} and 16.4% of Cr^{3+} ions were detected in the adsorbent.

The data of liquid medium analysis showed that nitrate anions do not participate in adsorption process, because after 30 min of experiment its concentration in liquid medium decreased less than 5%. Meanwhile, the measurements of calcium ions concentration showed that, after 30 s of adsorption, 88.0 mg (20.9%) of mentioned ions were released from the structure of the adsorbent in $Cu(NO_3)_2{\cdot}3H_2O$ solution (Fig. 5a). Moreover, unexpected results were obtained: after 1 min of adsorption, the amount of released Ca^{2+} ions decreased, while after 5 min, the equilibrium was attained and the number of released ions was equal to 115.6 mg (27.4%) (Fig. 5a). The same tendency was observed in $Cr(NO_3)_3{\cdot}9H_2O$ solution, although the amount of released Ca^{2+} ions was 1.31 times higher after 30 min of the experiment (Fig. 5b). It is worth mentioning that the amount of released Ca^{2+} ions tends to increase by increasing the duration of experiments when lower basicity calcium silicate hydrates are used for Me^{x+} adsorption [14].

The results show, that, after 30 min of Cu^{2+} adsorption, the exchange of $Cu^{2+} \leftrightarrow Ca^{2+}$ proceeded stoichiometric, while $Cr^{3+} \leftrightarrow Ca^{2+}$–non-stoichiometric. Presumably, it can be explained by the different valence or atomic radius between Ca^{2+} and adsorbed ions (Cr^{3+}, Cu^{2+}). According to the literature [32–33], the crystal structure of α-C_2SH consists of isolated $SiO_3(OH)$ tetrahedra, which share edges with $Ca(O,OH)_6$ and $Ca(O,OH)_7$ polyhedra. Thus, during the desorption of Ca^{2+} cations, OH^- anions are also released into the liquid medium. This fact was confirmed by the value of pH of a liquid medium, which increased from 2.99 (0 min)

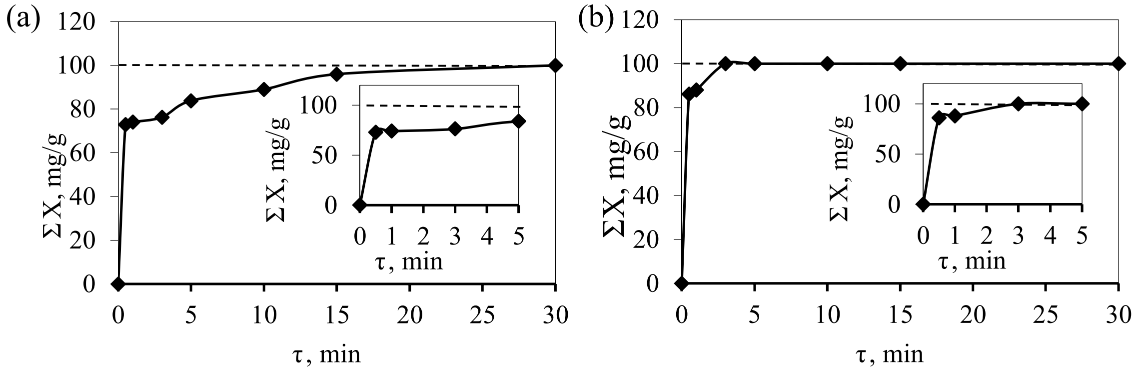

Fig. 4. Integral kinetic curve of Cu^{2+} (a) and Cr^{3+} (b) ions adsorption by α-C_2SH, when the initial concentration of ions was equal to 1 g/dm^3.

to 10.15 (30 min) in $Cr(NO_3)_3·9H_2O$ solution and from 4.72 (0 min) to 9.17 (30 min) in $Cu(NO_3)_2·3H_2O$ solution.

In order to determine kinetic parameters, the adsorption process was described by PFO and PSO equations. It was determined that PFO equation (Eq. (2)) did not fit the adsorption mechanism of Cu^{2+} and Cr^{3+} ions by the synthetic adsorbent because the error between the adsorbed ($q_{e(\exp)}$) and calculated ($q_{e(\mathrm{cal})}$) amount of Me^{x+} was higher than 5%–10% [52]. In addition to this, the values of correlation coefficients (R^2) were low (Table 3). However, different results were obtained by using PSO Eq. (4): the values of R^2 were equal to 0.99 (Table 3) and the relation between $q_{e(\exp)}$ and $q_{e(\mathrm{cal})}$ values was observed. Thus, it can be stated that a pseudo-second-order kinetics model adequately describes the Cu^{2+} and Cr^{3+} ions adsorption mechanism by α-C_2SH. It was calculated that the adsorption rate of Cr^{3+} ions (k_2 = 0.065 g/(mg min)) was approximately 3 times higher than Cu^{2+} (k_2 = 0.020 g/(mg min)). These results correspond to the experimental data because the adsorption process of Cr^{3+} ions ended after 3 min, while, in the case of Cu^{2+} ions,–after 30 min (Fig. 4). It should be noted that a pseudo-second-order kinetics model describes chemisorption, thus,

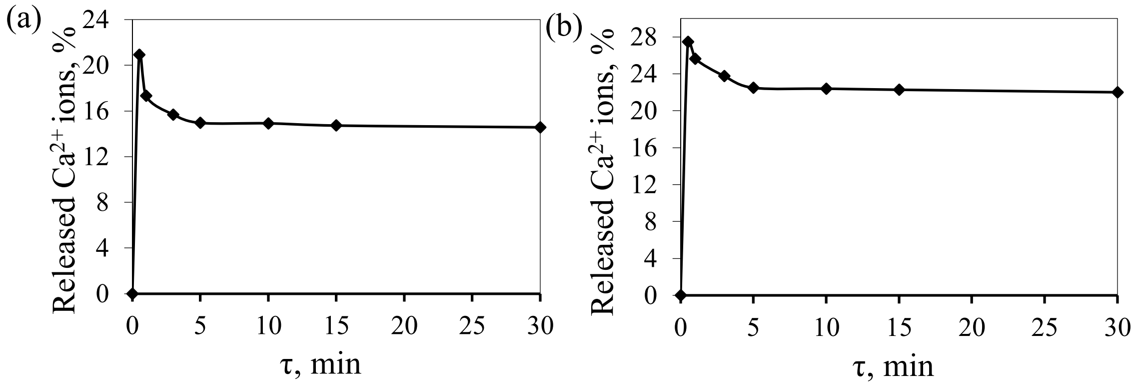

Fig. 5. Amount of released calcium ions from the adsorbent, when the initial concentration of Cu^{2+} (a) and Cr^{3+} (b) was equal to 1 g/dm^3.

Table 3
Kinetic parameters of the pseudo-first- and pseudo-second-order kinetic models

Metal ions	R^2	$q_{e(\exp)}$ (mg/g)	$q_{e(\mathrm{cal})}$ (mg/g)	k_1 (min^{-1})	k_2 (g/(mg min))
Pseudo-first-order kinetic models					
Cu^{2+}	0.813	100	42.89	0.156	–
Cr^{3+}	0.492	100	12.56	0.232	–
Pseudo-second-order kinetic models					
Cu^{2+}	0.99	100	95.45	–	0.020
Cr^{3+}	0.99	100	100.77	–	0.065

α-C_2SH acts more as a chemisorbent [53]. The same results can also be found in the literature [25,57].

XRD analysis data showed that α-C_2SH became metastable, since, after adsorption in $Cu(NO_3)_2{\cdot}3H_2O$ and $Cr(NO_3)_3{\cdot}9H_2O$ solutions, the intensity of this compound diffraction peaks decreased 1.1 and 2.3 times, respectively (Fig. 6). In the case of Cr^{3+} ions, the lower intensity of the aforementioned peaks can be explained by a higher amount of released Ca^{2+} ions from the structure of the adsorbent (Fig. 5). These results confirmed that heavy metal ions were adsorbed by α-C_2SH as there is no evidence of new compounds formation (metal hydroxides, metal oxides).

The previous results were also confirmed by the data of STA analysis. According to the literature [58], the first endothermic effect can be assigned to the dehydration of amorphous structure calcium silicate hydrates and/or removal of adsorption water. It was calculated that, after the adsorption, the mass loss and the heat of the mentioned thermal conversion increased two times (Fig. 7 and Table 4). Meanwhile, the endothermic effect in a 400°C–500°C temperature range describes the decompositions of α-C_2SH [58]:

$$2CaO{\cdot}SiO_2{\cdot}H_2O \rightarrow 2CaO{\cdot}SiO_2 + H_2O \tag{5}$$

According to the data of TGA, the adsorbent lost 5.25% of mass during the decomposition of α-C_2SH (Table 4), which is equivalent to 55.42% of α-C_2SH. It was determined that, after the adsorption, the amount of the mentioned compound decreased to 33.99% in $Cu(NO_3)_2{\cdot}3H_2O$ and 21.01% in $Cr(NO_3)_3{\cdot}9H_2O$ solutions (Fig. 7). These data were in good agreement with the results of Ca^{2+} desorption and XRD (Figs. 5 and 6). Meanwhile, in the case of Cu^{2+} ions, the increment in the intensity of the third endothermic effect confirmed that, during the adsorption experiments, carbonization proceeded

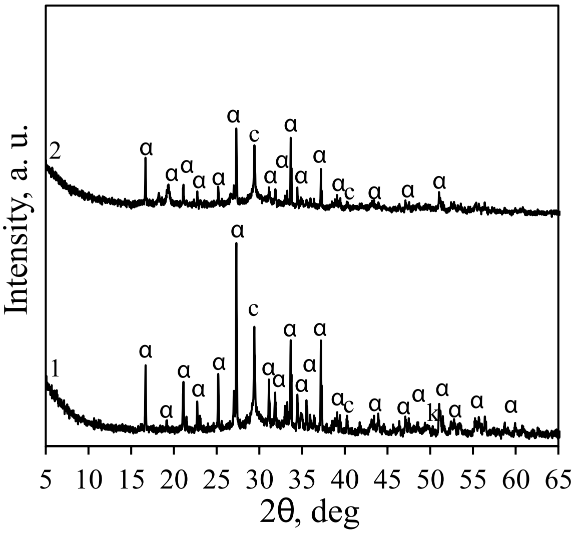

Fig. 6. XRD patterns of α-C_2SH after the adsorption in Cu^{2+} (Curve 1) and Cr^{3+} (Curve 2) solutions, when the initial concentration was equal to 1.00 g/cm³. Indices: α – α-C_2SH; c – $CaCO_3$; k – C-S-H(I)/C-S-H(II).

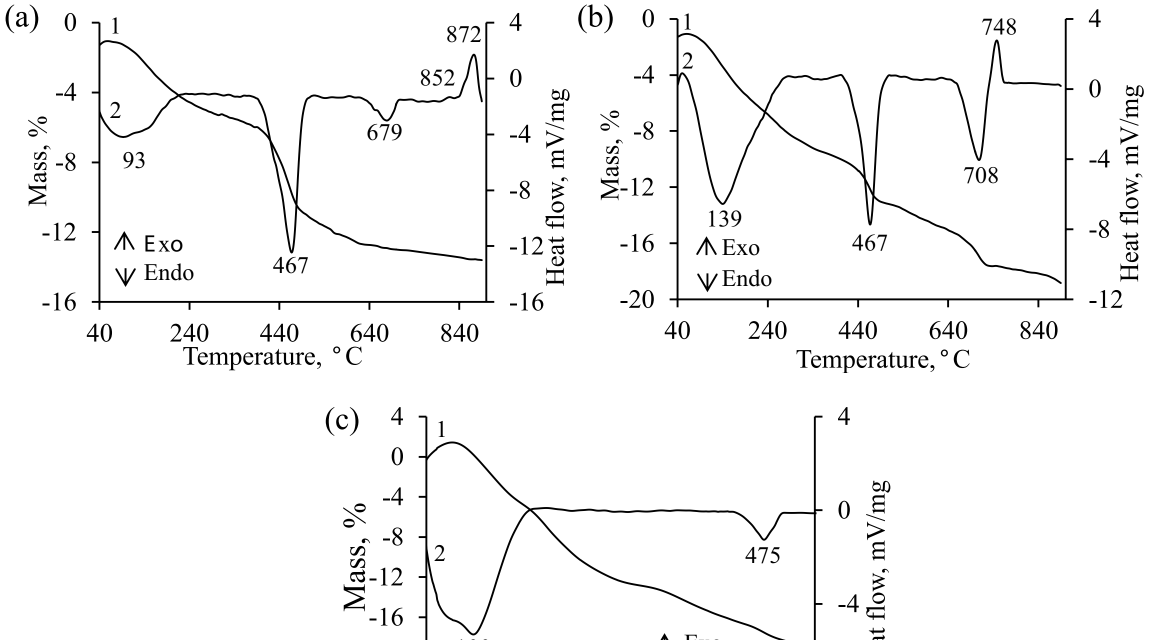

Fig. 7. STA curves (Curve 1 – TG; Curve 2 – DSC) of α-C_2SH after synthesis (a) and after adsorption in $Cu(NO_3)_2{\cdot}3H_2O$, (b) and in $Cr(NO_3)_3{\cdot}9H_2O$, and (c) solutions.

Table 4
Mass loss and the heat of the α-C_2SH after synthesis and adsorption process

	Mass loss, %							
	90°C–140°C		460°C–470°C		670°C–680°C		700°C–710°C	
	Δm, %	Q, J/g	Δm, %	Q, J/g	Δm, %	Q, J/g	Δm, %	Q, J/g
α-C_2SH	2.77	84	5.25	189	0.32	22	–	–
α-$C_2SH + Cu^{2+}$	5.43	153	3.22	145	–	–	2.33	61
α-$C_2SH + Cr^{3+}$	4.83	381	1.99	34	–	–	–	–

(Fig. 7). Additionally, an exothermic effect, which can be assigned to the recrystallization of semi-crystalline CSH, was shifted towards a higher temperature (Figs. 7a and b). It can be explained by the intercalation of Cu^{2+} ions or the decrement in crystallinity [59]. To avoid the interaction between Cr^{3+} ions and platinum crucibles, which were used for STA analysis, the experiment was carried out only at 540°C.

3.3. Adsorption experiments in 10.00 g Me^{x+}/dm^3 solution

In order to determine the maximum adsorption capacity of α-C_2SH for Cu^{2+} and Cr^{3+}ions, the concentration of these ions was increased to 10 g/dm^3. It was obtained that, at the beginning of Cu^{2+} ions adsorption (30 s), the adsorbed amount of the mentioned ions increased rapidly to 228.2 mg/g, and, after 30 min, it was equal to 615.54 mg/g (Fig. 8a). Meanwhile, in the case of Cr^{3+}ions adsorption, the removal efficiency was ~2.5 times lower and the number of incorporated ions was equal to 241.42 mg Cr^{3+}/g (Fig. 8b). During the adsorption, more than 50% of Ca^{2+} ions were released from the adsorbent into the liquid medium in both cases. Thus, it is not recommended to use α-C_2SH as a chemosorbent in the solutions containing more than 6 g Cu^{2+}/dm^3 and 2 g Cr^{3+}/dm^3 ions.

It was estimated that, after the adsorption experiments, α-C_2SH was fully decomposed, because the diffraction peaks typical to this compound were not detected in XRD patterns (Fig. 9a). It is worth mentioning that, in the copper nitrate solution, the precipitation of gerhardtite–$Cu_2(NO_3)(OH)_3$ (PDF04-011-9699) proceeded. The formation of this compound can be explained by a high concentration of OH^- anions, which were released with Ca^{2+} cations, and also low stability of metal ions in the alkaline medium. The formation of the mentioned compound was confirmed by STA data (Fig. 9b): at 237°C temperature, the decomposition of gerhardtite proceeded [60]:

$$4Cu_2(OH)_3NO_3 \rightarrow 8CuO + 4NO_2 + O_2 + 6H_2O \quad (6)$$

The endothermic effect at 400°C–500°C temperature, which is characteristic of α-C_2SH, was not observed (Fig. 9b).

Thus, synthetic α-C_2SH is a promising chemosorbent for the removal of heavy metal ions from the liquid medium since its adsorption capacity for Cu^{2+} and Cr^{3+} ions are 2–10 times higher than other adsorbents (hydrotalcite, CSH(I), zeolites) [27,61,62]. It should be noted that the adsorption process with the latter adsorbents proceeds 2–3 times slower in comparison with synthetic α-C_2SH [63]. According to the literature, gyrolite and some zeolites have high adsorption capacity (100–500 mg/g), however, after adsorption, these adsorbents become useless and are stored in a landfill [28,64]. In further research, α-C_2SH with incorporated Cu^{2+} and Cr^{3+} ions will be used for the production of alternative cementitious materials or as an additive in the production of OPC, and the properties of these binding materials such as hydration, mineralogical composition, and porosity will be examined.

4. Conclusions

- It was observed that the adsorption capacity of α-C_2SH, as well as the intercalation of heavy metals ions in its structure, depends on the chemical nature of the used

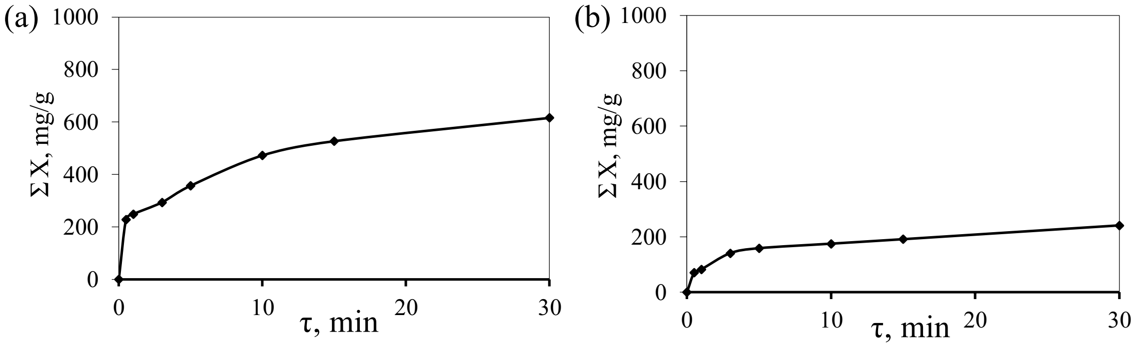

Fig. 8. Integral kinetic curve of Cu^{2+} (a) and Cr^{3+} (b) ions adsorption by α-C_2SH, when the initial concentration of ions was equal to 10 g/dm^3.

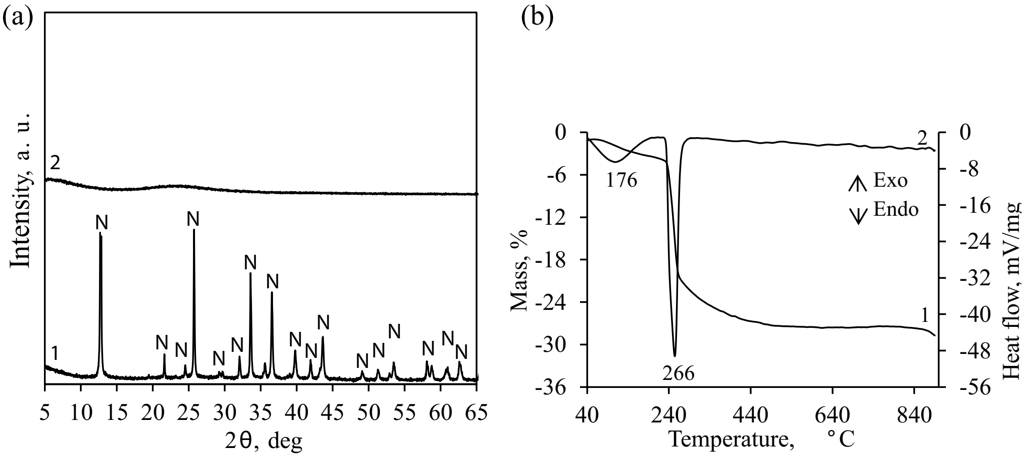

Fig. 9. XRD patterns (a) after the adsorption in Cu^{2+} (Curve 1) and Cr^{3+} (Curve 2) solutions and STA curves and (b) after the adsorption in Cu^{2+} solution, when initial concentration was equal to 10.00 g/cm^3. Indices: N – $Cu_2(NO_3)(OH)_3$.

adsorbate. Extremely high uptake of Cu^{2+} and Cr^{3+} ions was observed in 0.25 g Me^{x+}/dm^3 and 1 g Me^{x+}/dm^3 (where Me is Cu^{2+} or Cr^{3+} ions) concentration solutions. It was determined that the elimination yield of the mentioned ions is equal to 100%.

- The results showed that the adsorption process is not reversible in a neutral liquid medium because, after the desorption experiment, the concentration of Cu^{2+} and Cr^{3+} ions in the solution did not exceed ~0.01%. According to the kinetic calculations, it was proved that α-C_2SH acts as a chemisorbent and the adsorption rate in 1 g Cu^{2+}/dm^3 and 1 g Cr^{3+}/dm^3 solutions are equal to 0.02 and 0.065 g/(mg min), respectively. These data are in good agreement with the experimental results.
- It was determined that α-C_2SH is stable in the lowest concentration solutions, however, when the concentration of Me^{x+} ions was increased to 1 g/dm^3, the structure of the aforementioned compound was partially disrupted. Meanwhile, after the adsorption in 10 Me^{x+} g/dm^3 solutions, the crystal structure of α-C_2SH was fully destroyed and gerhardtite – $Cu_2(NO_3)(OH)_3$ were formed.

Acknowledgment

This research was funded by a grant (No. S-MIP–17-92) from the Research Council of Lithuania.

References

[1] P. Nagajyoti, K. Lee, T. Sreekanth, Heavy metals, occurrence and toxicity for plants: a review, Environ. Chem. Lett., 8 (2010) 199–216.
[2] Y. Hu, X. Liu, J. Bai, K. Shih, E.Y. Zeng, H. Cheng, Assessing heavy metal pollution in the surface soils of a region that had undergone three decades of intense industrialization and urbanization, Environ. Sci. Pollut. Res., 20 (2013) 6150–6159.
[3] L. El Fakir, M. Flayou, A. Dahchour, S. Sebbahi, F. Kifani-Sahban, S. El Hajjaji, Adsorptive removal of copper(II) from aqueous solutions on phosphates: equilibrium, kinetics, and thermodynamics, Desal. Wat. Treat., 57 (2016) 17118–17127.
[4] C. Canoluk, S.S. Gursoy, Chemical modification of rose leaf with polypyrrole for the removal of Pb(II) and Cd(II) from aqueous solution, J. Macromol. Sci. A, 54 (2017) 782–790.
[5] W. Shin, K. Na, Y. Kim, Adsorption of metal ions from aqueous solution by recycled aggregate: estimation of pretreatment effect, J. Ind. Eng. Chem., 57 (2016) 9366–9374.
[6] O.E.A. Salam, N.A. Reiad, M.M. ElShafei, A study of the removal characteristics of heavy metals from wastewater by low-cost adsorbents, J. Adv. Res., 2 (2011) 297–303.
[7] A. Bhatnagar, M. Sillanpää, Utilization of agro-industrial and municipal waste materials as potential adsorbents for water treatment—a review, Chem. Eng. J., 157 (2010) 277–296.
[8] S. Malamis, E. Katsou, A review on zinc and nickel adsorption on natural and modified zeolite, bentonite and vermiculite: examination of process parameters, kinetics and isotherms, J. Hazard. Mater., 252–253 (2013) 428–461.
[9] L. Giaccio, D. Cicchella, B. De Vivo, G. Lombardi, M. De Rosa, Does heavy metals pollution affects semen quality in men? A case of study in the metropolitan area of Naples (Italy), J. Geochem. Explor., 112 (2012) 218–225.
[10] M.M. Authman, M.S. Zaki, E.A. Khallaf, H.H. Abbas, Use of fish as bio-indicator of the effects of heavy metals pollution, J. Aquacult. Res. Dev., 6 (2015) 1–13.
[11] M. Barakat, New trends in removing heavy metals from industrial wastewater, Arabian J. Chem., 4 (2011) 361–377.
[12] M. Anjum, R. Miandad, M. Waqas, F. Gehany, M.A. Barakat, Remediation of wastewater using various nano-materials, Arabian J. Chem., 12 (2016) 1–23.
[13] C.Y. Cheok, N. Mohd Adzahan, R. Abdul Rahman, N.H. Zainal Abedin, N. Hussain, R. Sulaiman, G.H. Chong, Current trends of tropical fruit waste utilization, Crit. Rev. Food Sci. Nutr., 58 (2018) 335–361.
[14] J. Zhao, Y. Zhu, J. Wu, J. Zheng, X. Zhao, B. Lu, F. Chen, Chitosan-coated mesoporous microspheres of calcium silicate hydrate: environmentally friendly synthesis and application as a highly efficient adsorbent for heavy metal ions, J. Colloid Interface Sci., 418 (2014) 208–215.
[15] H.A. Hegazi, Removal of heavy metals from wastewater using agricultural and industrial wastes as adsorbents, HBRC J., 9 (2013) 276–282.
[16] A.M. Mahmoud, F.A. Ibrahim, S.A. Shaban, N.A. Youssef, Adsorption of heavy metal ion from aqueous solution by nickel oxide nano catalyst prepared by different methods, Egypt. J. Pet., 24 (2015) 27–35.
[17] E. Worch, Adsorption Technology in Water Treatment: Fundamentals, Processes, and Modeling, Walter de Gruyter Publications, Germany, 2012.

[18] T. Dambrauskas, K. Baltakys, J. Škamat, A. Kudžma, Hydration peculiarities of high basicity calcium silicate hydrate samples, J. Therm. Anal. Calorim., 131 (2018) 491–499.

[19] K. Baltakys, A. Eisinas, T. Dambrauskas, The influence of aluminum additive on the α-C2S hydrate formation process, J. Therm. Anal. Calorim., 121 (2015) 75–84.

[20] A. Ali, K. Saeed, Phenol removal from aqueous medium using chemically modified banana peels as low-cost adsorbent, Desal. Wat. Treat., 57 (2016) 11242–11254.

[21] S. He, C. Zhao, P. Yao, S. Yang, Chemical modification of silica gel with multidentate ligands for heavy metals removal, Desal. Wat. Treat., 57 (2016) 1722–1732.

[22] T.C. Drage, A. Arenillas, K.M. Smith, C.E. Snape, Thermal stability of polyethylenimine based carbon dioxide adsorbents and its influence on selection of regeneration strategies, Microporous Mesoporous Mater., 116 (2008) 504–512.

[23] V. Khandegar, A.K. Saroha, Electrocoagulation for the treatment of textile industry effluent – a review, J. Environ. Manage., 128 (2013) 949–963.

[24] Ihsanullah, A. Abbas, A.M. Al-Amer, T. Laoui, M.J. Al-Marri, M.S. Nasser, M. Khraisheh, M.A. Atieh, Heavy metal removal from aqueous solution by advanced carbon nanotubes: critical review of adsorption applications, Sep. Purif. Technol., 157 (2016) 141–161.

[25] V. Kasperaviciute, K. Baltakys, R. Siauciunas, The sorption properties of gyrolite for copper ions, Ceram. Silik., 52 (2008) 95–101.

[26] A. Bankauskaite, K. Baltakys, A. Eisinas, S. Zadaviciute, A study on the intercalation of heavy metal ions in a wastewater by synthetic layered inorganic adsorbents, Desal. Wat. Treat., 56 (2015) 1576–1586.

[27] Q. Chen, C.D. Hills, M. Yuan, H. Liu, M. Tyrer, Characterization of carbonated tricalcium silicate and its sorption capacity for heavy metals: a micron-scale composite adsorbent of active silicate gel and calcite, J. Hazard. Mater., 153 (2008) 775–783.

[28] S.S. Obaid, D.K. Gaikwad, M.I. Sayyed, K. AL-Rashdi, P.P. Pawar, Heavy metal ions removal from wastewater by the natural zeolites, Mater. Today:. Proc., 5 (2018) 17930–17934.

[29] O. Shrivastava, F.P. Glasser, Ion-exchange properties of $Ca_5Si_6O_{18}H_2·4H_2O$, J. Mater. Sci. Lett., 4 (1985) 1122–1124.

[30] N. Labhasetwar, O. Shrivastava, $Ca_2 \rightleftharpoons Pb_2$ exchange reaction of calcium silicate hydrate: $Ca_5Si_6O_{18}H_2·4H_2O$, J. Mater. Sci., 24 (1989) 4359–4362.

[31] L. Skinner, S. Chae, C. Benmore, H. Wenk, P. Monteiro, Nanostructure of calcium silicate hydrates in cements, Phys. Rev. Lett., 104 (2010) 195502.

[32] E. Gartner, H. Hirao, A review of alternative approaches to the reduction of CO_2 emissions associated with the manufacture of the binder phase in concrete, Cem. Concr. Res., 78 (2015) 126–142.

[33] K. Okano, S. Miyamaru, A. Kitao, H. Takano, T. Aketo, M. Toda, K. Honda, H. Ohtake, Amorphous calcium silicate hydrates and their possible mechanism for recovering phosphate from wastewater, Sep. Purif. Technol., 144 (2015) 63–69.

[34] W. You, M. Hong, H. Zhang, Q. Wu, Z. Zhuang, Y. Yu, Functionalized calcium silicate nanofibers with hierarchical structure derived from oyster shells and their application in heavy metal ions removal, Phys. Chem. Chem. Phys., 18 (2016) 15564–15573.

[35] S. Shaw, S.M. Clark, C.M.B. Henderson, Hydrothermal formation of the calcium silicate hydrates, tobermorite ($Ca_5Si_6O_{16}(OH)_2·4H_2O$) and xonotlite ($Ca_6Si_6O_{17}(OH)_2$): an in situ synchrotron study, Chem. Geol., 167 (2000) 129–140.

[36] J.J. Chen, J.J. Thomas, H.F.W. Taylor, H.M. Jennings, Solubility and structure of calcium silicate hydrate, Cem. Concr. Res., 34 (2004) 1499–1519.

[37] C. Labbez, A. Nonat, I. Pochard, B. Jönsson, Experimental and theoretical evidence of overcharging of calcium silicate hydrate, J. Colloid Interface Sci., 309 (2007) 303–307.

[38] I.G. Richardson, The calcium silicate hydrates, Cem. Concr. Res., 38 (2008) 137–158.

[39] Q.Y. Chen, M. Tyrer, C.D. Hills, X.M. Yang, P. Carey, Immobilisation of heavy metal in cement-based solidification/stabilization: a review, Waste Manage., 29 (2009) 390–403.

[40] R. Siauciunas, K. Baltakys, R. Gendvilas, A. Eisinas, The influence of Cd-impure gyrolite on the hydration of composite binder material based on α-C_2S hydrate, J. Therm. Anal. Calorim., 118 (2014) 857–863.

[41] X. Guo, H. Shi, Microstructure and heavy metal adsorption mechanisms of hydrothermally synthesized Al-substituted tobermorite, Mater. Struct., 50 (2017) 245.

[42] K. Baltakys, A. Eisinas, I. Barauskas, E. Prichockiene, E. Zaleckas, Removal of Zn(II), Cu(II) and Cd(II) from aqueous solution using gyrolite., J. Sci. Ind. Res., 71 (2012) 566–572.

[43] S. Zadaviciute, A. Bankauskaite, K. Baltakys, A. Eisinas, The study of CP determination of hydrotalcite intercalated with heavy metal ions, J. Therm. Anal. Calorim., 131 (2018) 521–527.

[44] S. Chen, C. Cheng, C. Li, P. Chai, Y. Chang, Reduction of chromate from electroplating wastewater from pH 1 to 2 using fluidized zero-valent iron process, J. Hazard. Mater., 142 (2007) 362–367.

[45] P. Miretzky, A.F. Cirelli, Cr(VI) and Cr(III) removal from aqueous solution by raw and modified lignocellulosic materials: a review, J. Hazard. Mater., 180 (2010) 1–19.

[46] A.Z.M. Badruddoza, Z.B.Z. Shawon, W.J.D. Tay, K. Hidajat, M.S. Uddin, Fe_3O_4/cyclodextrin polymer nanocomposites for selective heavy metals removal from industrial wastewater, Carbohydr. Polym., 91 (2013) 322–332.

[47] A. Heidari, H. Younesi, Z. Mehraban, Removal of Ni(II), Cd(II), and Pb(II) from a ternary aqueous solution by amino functionalized mesoporous and nano mesoporous silica, Chem. Eng. J., 153 (2009) 70–79.

[48] S. Sen Gupta, K.G. Bhattacharyya, Kinetics of adsorption of metal ions on inorganic materials: a review, Adv. Colloid Interface Sci., 162 (2011) 39–58.

[49] M. Algarra, M.V. Jiménez, E. Rodríguez-Castellón, A. Jiménez-López, J. Jiménez-Jiménez, Heavy metals removal from electroplating wastewater by aminopropyl-Si MCM-41, Chemosphere, 59 (2005) 779–786.

[50] D. Niuniavaite, K. Baltakys, T. Dambrauskas, The adsorption kinetic parameters of Co_2 ions by α-C_2SH, Buildings, 8 (2018) 10.

[51] J.H. Johnston, T. Borrmann, D. Rankin, M. Cairns, J.E. Grindrod, A. Mcfarlane, Nano-structured composite calcium silicate and some novel applications, Curr. Appl. Phys., 8 (2008) 504–507.

[52] J. Lin, L. Wang, Comparison between linear and non-linear forms of pseudo-first-order and pseudo-second-order adsorption kinetic models for the removal of methylene blue by activated carbon, Front. Environ. Sci. Eng., 3 (2009) 320–324.

[53] J. Simonin, On the comparison of pseudo-first-order and pseudo-second-order rate laws in the modeling of adsorption kinetics, Chem. Eng. J., 300 (2016) 254–263.

[54] A.A. Inyinbor, F.A. Adekola, G.A. Olatunji, Kinetics, isotherms and thermodynamic modeling of liquid phase adsorption of Rhodamine B dye onto *Raphia hookerie* fruit epicarp, Water Resour. Ind., 15 (2016) 14–27.

[55] S. Azizian, Kinetic models of sorption: a theoretical analysis, J. Colloid Interface Sci., 276 (2004) 47–52.

[56] Y.S. Ho, G. McKay, Pseudo-second-order model for sorption processes, Process Biochem., 34 (1999) 451–465.

[57] S. Zadaviciute, K. Baltakys, A. Eisinas, A. Bankauskaite, Simultaneous adsorption at 25°C and the peculiarities of gyrolite substituted with heavy metals, J. Therm. Anal. Calorim., 127 (2017) 335–343.

[58] S. Shaw, C.M.B. Henderson, B.U. Komanschek, Dehydration/recrystallization mechanisms, energetics, and kinetics of hydrated calcium silicate minerals: an in situ TGA/DSC and synchrotron radiation SAXS/WAXS study, Chem. Geol., 167 (2000) 141–159.

[59] J. Gong, T. Liu, X. Wang, X. Hu, L. Zhang, Efficient removal of heavy metal ions from aqueous systems with the assembly of anisotropic layered double hydroxide nanocrystals@ carbon nanosphere, Environ. Sci. Technol., 45 (2011) 6181–6187.

[60] D.C. Pereira, D.L.A. de Faria, V.R. Constantino, Cu^{II} hydroxy salts: characterization of layered compounds by vibrational spectroscopy, J. Braz. Chem. Soc., 17 (2006) 1651–1657.

[61] Z. Wang, K. Tan, J. Cai, S. Hou, Y. Wang, P. Jiang, M. Liang, Silica oxide encapsulated natural zeolite for high-efficiency removal of low concentration heavy metals in water, Colloids Surf., A, 561 (2019) 388–394.

[62] F. Ogata, E. Ueta, N. Kawasaki, Characteristics of a novel adsorbent Fe–Mg-type hydrotalcite and its adsorption capability of As(III) and Cr(VI) from aqueous solution, J. Ind. Eng. Chem., 59 (2018) 56–63.

[63] T. Link, F. Bellmann, H. Ludwig, M.B. Haha, Reactivity and phase composition of Ca2SiO4 binders made by annealing of alpha-dicalcium silicate hydrate, Cem. Concr. Res., 67 (2015) 131–137.

[64] X. Guo, F. Meng, H. Shi, Microstructure and characterization of hydrothermal synthesis of Al-substituted tobermorite, Constr. Build. Mater., 133 (2017) 253–260.